Scientific Works of Azerbaijan University of Architecture and Construction, 2026, N1
www.swjournal.az

Elmi Əsərlər Jurnalı Azərbaycan Memarlıq və İnşaat Universiteti, 2026, N1
sw@azmiu.edu.az

https://doi.org/10.58225/sw.2026.1-15-24

EFFECT OF GAMMA IRRADIATION AND THERMAL ANNEALING ON THE STRUCTURAL AND DEFECT PROPERTIES OF ZRB₂ CERAMICS

Samadov Samir[1*], Nguyen Minh Trung[1,2], Popov Evgeni[1,3], Sidorin Anatoliy[1]
[1]Joint Institute for Nuclear Research, Dubna, 141980, Russia*
[2]Institute of Physics, Vietnam Academy of Science and Technology, Hanoi, 10000, Vietnam
[3]Institute of Catalysis, Bulgarian Academy of Sciences, Sofia, 1113, Bulgaria
samirsamedov@jinr.ru

Abstract. This work examines the influence of gamma irradiation and subsequent thermal annealing on the structural and defect-related properties of zirconium diboride (ZrB_2) nanocrystals. The samples were irradiated with absorbed doses of 1500 and 3000 kGy and analyzed by X-ray diffraction, Fourier-transform infrared spectroscopy, positron annihilation lifetime spectroscopy, and Doppler broadening spectroscopy. The results showed that ZrB_2 preserved its hexagonal structure without the formation of secondary phases, confirming its high radiation stability. At the same time, small shifts in diffraction peaks, slight lattice expansion, and changes in FTIR bands indicated local structural distortions and surface oxidation processes. Positron annihilation measurements revealed irradiation-induced modification of vacancy-type defects and redistribution of positron trapping centers. Electron momentum analysis also confirmed changes in the local electronic structure after irradiation. Overall, ZrB_2 demonstrates high resistance to gamma irradiation, while exhibiting limited but detectable structural and defect evolution.
Keywords: ZrB_2 ceramics; gamma irradiation; X-ray diffraction; PAS; vacancy-type defects

Cite this article as: *S. Samadov, N. M. Trung, E. Popov, and A. Sidorin, "EFFECT OF GAMMA IRRADIATION AND THERMAL ANNEALING ON THE STRUCTURAL AND DEFECT PROPERTIES OF ZrB_2 CERAMICS", SW AzUAC, vol. 1, 2026, doi:10.58225/sw.2026.1-15-24*
Article history: *Received: 14 January 2026 / Revised: 20 February 2026 / Accepted: 04 March 2026*

1. Introduction. Zirconium diboride (ZrB_2) is one of the most promising ultra-high-temperature ceramic materials due to its high melting point, excellent thermal and electrical conductivity, high hardness, as well as strong resistance to chemical attack and corrosive environments. Owing to this combination of properties, ZrB_2 has attracted considerable interest for applications in aerospace technology, nuclear engineering, protective coatings, high-temperature electrodes, and other fields where structural stability is required under severe external conditions [1-3]. In particular, its resistance to thermal effects and irradiation makes ZrB_2 a promising material for components operating under extreme service conditions.

In recent years, interest in the behavior of ZrB_2 under the influence of external factors such as temperature, pressure, and various types of radiation has increased significantly. Previous studies have shown that irradiation with heavy ions, neutrons, and electrons can induce measurable changes in the lattice parameters, defect structure, degree of amorphization, and local atomic arrangement in zirconium diboride [4-6]. However, the hexagonal crystal structure of ZrB_2 is largely preserved in most cases, indicating a high structural stability of the material. Previous studies based on X-ray diffraction have also shown that irradiation can induce lattice expansion, local disorder, and limited amorphization [7-8]. While these results confirm that ZrB_2 is a structurally stable material, they also indicate that its response is strongly dependent on the irradiation conditions and subsequent thermal history.

However, the effect of high-dose gamma irradiation on the structural and defect evolution in ZrB_2 remains insufficiently understood, particularly when crystallographic and defect-sensitive techniques are applied in a combined manner. Conventional structural methods such as X-ray diffraction provide important information on phase composition, lattice deformation, and long-range order, while FTIR spectroscopy is useful for identifying changes in surface bonding, oxidation-related groups, and local chemical environments induced by irradiation [9, 10]. However, these techniques alone are not sufficient to fully reveal the evolution of vacancy-type defects and the redistribution of local electron density in irradiated ceramics. In this context, positron annihilation techniques are of particular importance, as positron lifetime and Doppler broadening parameters exhibit high sensitivity to vacancies, vacancy clusters, open-volume defects, and changes in the electronic environment [11]. Previous PAS-based studies on ZrB_2 have shown that gamma irradiation can significantly alter the size and distribution of vacancy-related defects.

Therefore, a comprehensive approach combining XRD, FTIR, positron annihilation lifetime spectroscopy, Doppler broadening spectroscopy, and electron momentum distribution analysis is essential for a more complete interpretation of irradiation-induced changes in ZrB_2. Such an approach enables the correlation between long-range structural stability and local bond rearrangement, defect formation, and modifications in the electronic structure. In the present study, ZrB_2 powder samples were subjected to gamma irradiation at absorbed doses of 1500 and 3000 kGy. The primary objective of this work is to clarify the effects of gamma irradiation on the crystal structure, surface chemical state, vacancy-type defects, and electron momentum characteristics of ZrB_2.

2. Materials and Methods. The zirconium diboride (ZrB_2) material employed in this study possesses a hexagonal crystal structure, a particle size below 3 μm, and a purity level of 99%. Gamma irradiation of the samples was conducted using a ^{60}Co source in the Gamma MRX-25 facility at the Institute of Radiation Problems, Ministry of Science and Education of Azerbaijan. The irradiation was performed at room temperature with two different absorbed doses, namely 1500 kGy and 3000 kGy. During the process, the source activity was 4160 Ci, and the dose rate was maintained at 6.05 Gy/s.

The crystal structure, phase composition, texture, and grain size of the samples were investigated using X-ray diffraction (XRD) analysis. The measurements were carried out with a PANalytical EMPYREAN diffractometer employing Cu Kα radiation (λ = 1.5405 nm). Data collection was performed in $\theta/2\theta$ scanning geometry over the 20–100° angular range, with a step size of 0.02° and a scanning rate of 1° per minute. The incident angle was fixed at 3°, and all analyses were conducted at room temperature [12].

A Varian 640-IR Fourier-transform infrared spectrometer (FTIR) was employed to investigate the chemical bonding and functional groups in zirconium diboride (ZrB_2) powders subjected to gamma irradiation and subsequent thermal treatment [13]. For sample preparation, ZrB_2 was thoroughly mixed with potassium bromide (KBr) in a mass ratio of 1:300, and pellets with a thickness of 3–7 μm and dimensions of 8.0 × 30 mm² were formed at room temperature under a pressure of 6.0×10^4 N/m². The FTIR measurements were carried out over a spectral range up to 1800 cm^{-1}. All data were acquired under controlled experimental conditions, and the resulting spectra were systematically analyzed to evaluate structural modifications induced by gamma irradiation and thermal exposure.

Positron lifetime measurements were carried out using a fast–fast coincidence spectrometer equipped with BaF_2 scintillation detectors. The instrument provided a time resolution of 260 ps (FWHM). A ^{22}Na positron source with an activity of 6.5 μCi, encapsulated in a 7 μm thick titanium foil, was placed between two identical specimens in a sandwich-like arrangement. This configuration was positioned in front of the detectors of the lifetime spectrometer. To ensure sufficient statistical accuracy, data acquisition was performed over a 24-hour period, yielding more than $\sim 3 \times 10^6$ counts. The recorded spectra were analyzed using the LT software package [14].

For Doppler broadening investigations, a slow positron beam system derived from a positron injector component was utilized. The experimental setup was installed and operated at the Joint Institute for Nuclear Research. Doppler Broadening Spectroscopy (DBS) measurements were conducted using a high-purity germanium (HPGe) detector with an energy resolution of about 511 ±

1.2 keV, enabling accurate detection of annihilation gamma photons. Signal processing was supported by a preamplifier and amplifier chain. The Doppler spectra were evaluated in terms of the S and W shape parameters, and the obtained data were calibrated with the SP-SE software [15].

3. Results and Discussion

3.1. Effect of gamma irradiation on the crystal structure of zirconium diboride

Figure 1 presents the X-ray diffraction patterns of ZrB_2 nanocrystals subjected to gamma irradiation at different absorbed doses. Comparative analysis of the spectra indicates that although some changes occur in the crystal structure with increasing absorbed dose, no formation of new phases or oxide phases is observed. This demonstrates the high radiation resistance of the material. Structural analysis performed using the Rietveld method determined the lattice parameters of ZrB_2 nanocrystals as a = 3.16846 Å, c = 3.53042 Å, and the unit cell volume V = 30.694 Å^3. The obtained results are in good agreement with literature data, confirming the high crystallinity of the synthesized material [16]. A more detailed analysis of the diffraction peaks shows that, particularly for the peaks indexed to the (101) plane, small but systematic shifts along the abscissa axis occur with increasing absorbed dose. Such shifts are associated with changes in lattice parameters and indicate the formation of local distortions in the crystal lattice under irradiation. These local deformations cause partial degradation in the columnar structural elements, leading to the onset of a weak amorphization process in the material. Calculations reveal that at absorbed doses of 300 kGy, 1000 kGy, 1500 kGy, and 3000 kGy, the maximum degree of amorphization is approximately 1.2%. This implies that the material largely preserves its crystalline structure, with disorder appearing only in limited regions [17].

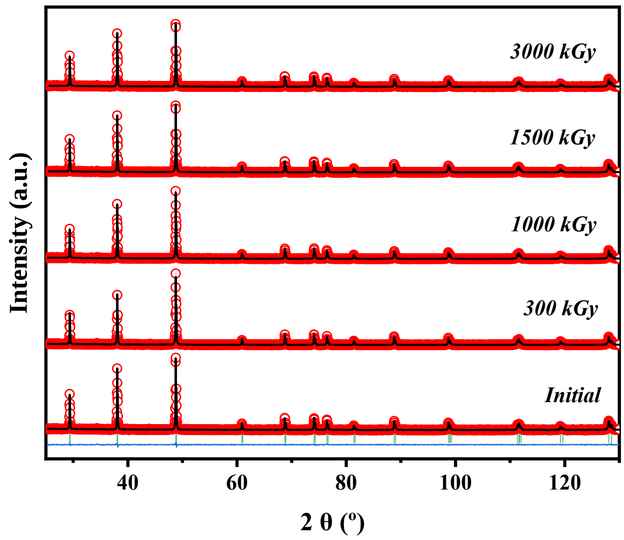

Fig. 1. Diffraction spectra of ZrB_2 nanocrystals irradiated at different absorbed doses. The lattice parameters of the ZrB_2 nanocrystal were determined as a = 3.16846 Å, c = 3.53042 Å, and V = 30.694 Å^3

On the other hand, internal stresses generated within the lattice due to gamma irradiation lead to an expansion of the crystal structure. Analysis of the lattice volume variation shows that at a dose of 300 kGy, the volume remains nearly stable. However, at doses of 1000 kGy and 1500 kGy, a sharp increase in volume is observed. At a higher dose of 3000 kGy, this increase ceases and reaches a stationary state (Fig. 2). This behavior is characteristic of ceramic-based materials and can be explained by the fact that lattice expansion under radiation reaches a maximum and then stabilizes [18]. For ZrB_2 nanocrystals, the maximum lattice volume expansion was determined to be $\Delta V = 0.011$ Å^3. These results indicate that even under high-dose irradiation conditions, the material largely maintains its structural integrity, undergoing only minor structural modifications.

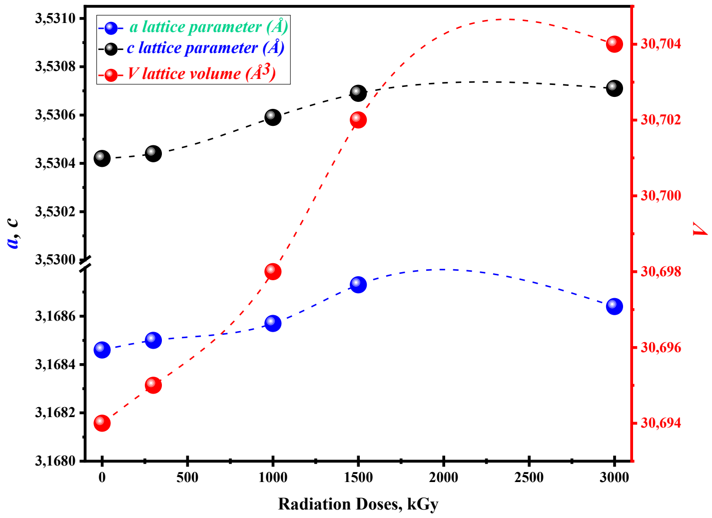

Fig. 2. Variation behavior of lattice parameters in zirconium diboride nanocrystals under gamma irradiation

These XRD results indicate that gamma irradiation does not induce phase transformation in ZrB_2, but it produces slight lattice distortions and limited disorder within the crystal structure. However, XRD mainly reflects long-range structural changes; therefore, to better understand irradiation-induced modifications in surface bonding and local chemical states, FTIR analysis was performed.

3.2. FTIR analysis of zirconium diboride under high gamma irradiation and after thermal annealing

Figure 3 presents the FTIR spectra of zirconium diboride samples before and after thermal treatment at 1173 K, following irradiation at doses of 1500 and 3000 kGy. In the spectrum of the non-irradiated ZrB_2 ceramic, vibrational modes corresponding to chemical bonds are detected at wavenumbers of approximately 650 cm^{-1}, 750 cm^{-1}, 838 cm^{-1}, and 3435 cm^{-1}. These observations are in good agreement with previously reported FTIR studies on ZrB_2-based composites and materials synthesized via sol–gel and carbothermal reduction methods [19], [20].

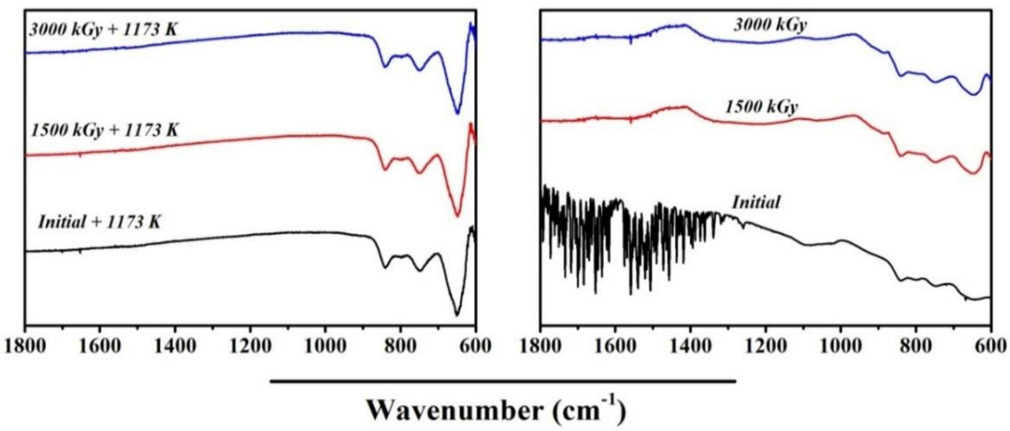

Fig. 3. Fourier transform infrared spectroscopy spectra of the ZrB_2 crystal at different gamma absorption doses and thermal annealing

With increasing irradiation dose (1500 and 3000 kGy), a noticeable enhancement in the intensity of all identified vibrational bands is observed. The FTIR analysis suggests that gamma irradiation promotes the formation of active sites on the surface of zirconium diboride, facilitating the development of additional oxide-related centers. Furthermore, the results indicate the effective decomposition of hydroxyl and other functional groups present on the surface.

At an irradiation dose of 3000 kGy, the intensities of all peaks in the treated sample become nearly uniform. In unirradiated ZrB_2, the band at ~646 cm^{-1} is assigned to symmetric Zr–O–Zr stretching, while the peak at ~754 cm^{-1} corresponds to asymmetric vibrations. Zr–O bonds are typically observed within the 400–700 cm^{-1} range, although overlapping modes such as ν(Zr–O) + ν(Zr–N) and π(C–CH_3) + ν(Zr–O) with ring distortion may also contribute in this region [21]. The band near 839 cm^{-1} is attributed to ν(Zr–O–C) stretching [22], and the peak at 1287 cm^{-1} corresponds to ν(B=O) vibrations. Since the samples were irradiated under ambient conditions, surface transformations are likely to occur through several mechanisms.

$$ZrB_2(active\ surface) \xrightarrow{\gamma\ radiation} ZrB^{n+}\ (active\ centers: H^{\cdot}, HO^{\cdot}, O^{\cdot}) + H_2O \times B(OH)_3$$

The mechanism of decomposition of water molecules absorbed by the surface of the sample as a result of the action of gamma radiation is given in the following equations.

$$H_2O \times B(OH)_3 \xrightarrow{\gamma\ radiation} B(OH)_4^+ + H^- + B - O$$

$$H_2O \xrightarrow{\gamma\ radiation} H_2O^{\cdot+} + e^-$$

Following thermal treatment, the FTIR spectra exhibit increased intensities at 650, 750, and 838 cm^{-1}, indicating enhanced bond vibrations along with the complete decomposition of hydroxyl and related functional groups. Oxygen species interacting with active Zr sites lead to the formation of Zr–O–Zr and Zr–O–C bonds, confirming surface oxidation. Under ambient irradiation conditions, free radicals facilitate the generation of oxidized functional groups, whose concentration increases with higher gamma radiation doses.

The unchanged vertical slope of the “shoulder” in the broadened peaks across all frequencies suggests a uniform interaction between the active surface and oxygen. Additionally, the concentration of oxide centers on the ZrB_2 surface increases with increasing radiation dose. The FTIR results complement the XRD findings by showing that, although the bulk crystal structure remains preserved, irradiation promotes surface-related chemical modification and oxidation-related bond formation. Since these structural and chemical changes are expected to affect vacancy-type defects and local electron-density distribution, positron annihilation techniques were further applied to examine the defect evolution in greater detail.

3.3. Effect of Gamma Irradiation on Positron Annihilation Parameters in ZrB_2

Positron annihilation lifetime spectroscopy (PALS) measurements were performed to conduct a comparative analysis of the samples before and after gamma irradiation. For each sample, two lifetime components (τ_1 and τ_2) along with their corresponding relative intensities (I_1 and I_2) were determined. Table 1 presents the lifetime components and their relative intensities obtained for zirconium diboride samples after gamma irradiation.

Table 1. Lifetime components and relative intensities of zirconium diboride samples after gamma irradiation

Parameters	initial	1500 kGy	3000 kGy
τ_{mean} (ns)	0.188	0.190	0.193
I_2 (%)	24.5	21.2	16.0
I_1 (%)	75.5	78.8	84.0
τ_2 (ns)	0.232	0.246	0.261
τ_1 (ns)	0.174	0.176	0.181

These lifetime components reflect different electronic environments and interaction mechanisms within the material. The PALS results indicate that these parameters provide important information about defects, vacancies, and the overall electron density distribution in the crystal structure [23]. In general, the τ_1 component is mainly associated with bulk annihilation processes and small vacancy-type complexes. The increase of this component from 174±2 ps to 181±1 ps suggests that irradiation induces changes in the electron density and in positron–electron interaction conditions within the material. These variations can be explained by the formation of vacancy-type defects or the reconfiguration of pre-existing defect structures.

The τ_2 component is predominantly related to positron annihilation at grain boundaries and within vacancy clusters [24]. After gamma irradiation, this component increases from 232 ± 5 ps to 261 ± 8 ps, indicating the formation of larger defect complexes. At the same time, the decrease in the I_2 intensity from 24.5% to 16% suggests a change in the relative contribution of these defect-related states, which may be associated with a reduction in their population or a redistribution of defect structures. Within the framework of the single-defect trapping model, variations in I_2 are linked to structural changes reflected in the primary lifetime parameters τ_1 and τ_2. Conversely, I_1 increases from 75.5% to 84.0%, indicating a higher contribution of bulk-like or monovacancy-related states to the annihilation process. Overall, the results demonstrate that gamma irradiation significantly modifies the defect structure of ZrB_2 and leads to a redistribution of positron trapping centers within the material.

The effect of gamma irradiation was investigated using variable-energy positron beams, and the results are presented in Fig. 1 (see supplementary materials for details). In both unirradiated and irradiated samples, the S parameter decreases with increasing annihilation depth. An increase in gamma dose leads to a higher concentration of open-volume defects in ZrB_2. For low-energy positrons (0–5 keV, up to ~0.23 µm depth), the elevated S parameter is attributed to enhanced surface annihilation. At higher energies (>10 keV), most positrons annihilate within the bulk of the material. In general, the increase in the S parameter reflects the growing contribution of both surface and bulk defects, indicating an overall rise in defect density. The pronounced increase observed in the 5–10 keV range after a dose of 1500 kGy is likely associated with changes in the electronic structure related to boron vacancies.

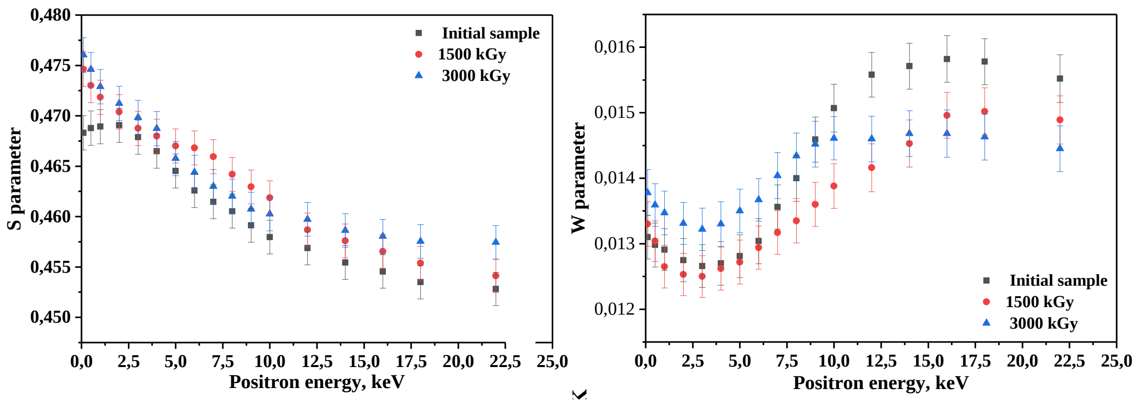

Fig. 4. Positron energy dependence of the S and W parameters for ZrB2 samples exposed to gamma radiation. On the left is the S-E dependence (S- characterizes the low momentum field), on the right is the W-E dependence (W- characterizes the high momentum field)

The combined analysis of the S and W parameters suggests that their variation may indicate positronium formation in regions with low electron density [25], [26]. According to the PLT results, in unannealed samples, the contribution of annihilation in intergranular regions increases with gamma dose, implying the possible formation of long-lived components. In contrast, annealed ZrB_2 samples tend to reach a more stable structural state at higher doses, approaching stoichiometric equilibrium.

This behavior indicates a transition toward a lower entropy state and suggests that, with annealing, the material can maintain its functional properties at gamma doses below 3000 kGy.

3.4. Electron Momentum Distribution in Gamma-Irradiated ZrB_2

The electron momentum distribution (EMD) spectra of gamma-irradiated ZrB_2 nanocrystals at a positron energy of 12 keV are presented in Figure 5. Preliminary analysis reveals the formation of approximately three main peaks corresponding to the degeneracy of electronic energy levels along the depth, with their intensities determined by the overlap of positron–electron wave functions. Similar peak structures have also been reported in other zirconium-based materials [27]. A comparison of peak positions shows that with increasing gamma irradiation dose, the peaks systematically shift toward higher momentum values (to the right). Specifically, the first peak, located at ~10.49×10^{-3} m_0c in the unirradiated sample, shifts to ~11×10^{-3} m_0c at the maximum dose, while the second peak moves from ~12.2×10^{-3} m_0c to ~13.4×10^{-3} m_0c. At an absorbed dose of 3000 kGy, a noticeable decrease in peak intensity is observed, which is associated with an increase in defect concentration [28].

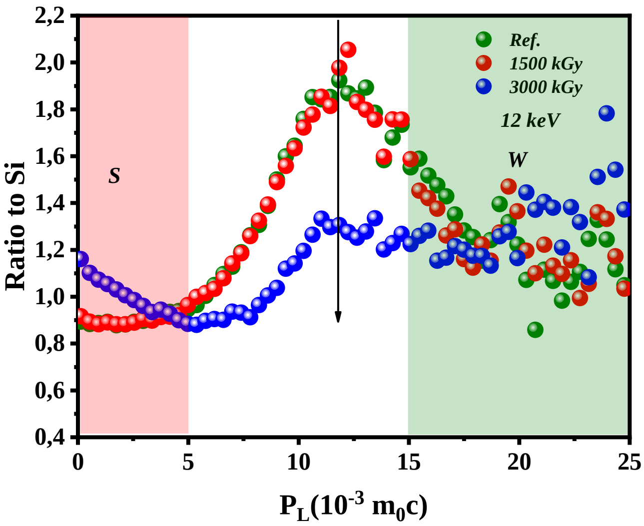

Fig. 5. Influence of gamma irradiation on the electron momentum distribution (EMD) spectra of zirconium diboride samples

Changes observed in the low-momentum region (~4×10^{-3} m_0c) are mainly attributed to open-volume defects acting as positron trapping centers, and the increase in intensity in this region indicates the formation of such defects [29]. The EMD spectra of ZrB_2 exhibit features characteristic of boron-based systems and are consistent with the results reported by Pujari et al. [30]. A significant fraction of positrons annihilates within the boron sublattice, which can be explained by the tendency of boron atoms to gain electrons from the metal matrix and become negatively charged [31]. From an electronic structure perspective, the overall electron density in the Zr–B system is mainly governed by the hybridization of Zr-4d and B-2p orbitals. However, irradiation-induced defects modify this interaction, leading to a redistribution of electronic states in both valence and core regions, which is reflected in the observed changes in the EMD spectra.

Overall, the combined results obtained from XRD, FTIR, PALS/DBS, and EMD demonstrate a consistent picture of irradiation-induced modification in ZrB_2. XRD shows that the material preserves its hexagonal phase with only minor lattice distortion and weak amorphization. FTIR reveals that these structural changes are accompanied by surface oxidation and bond rearrangement. Positron annihilation measurements confirm that gamma irradiation alters the concentration and nature of vacancy-type defects and positron trapping centers, while the EMD spectra indicate that these defects also affect the local electronic structure through redistribution of electron momentum. Therefore, all applied methods consistently show that gamma irradiation does not destroy the structural framework of ZrB_2, but induces limited and measurable evolution at the crystallographic, defect, chemical, and electronic levels.

4. Conculusion. In this work, the influence of gamma irradiation and post-irradiation thermal annealing on zirconium diboride nanocrystals was comprehensively studied using XRD, FTIR, PALS, and DBS methods. The obtained results demonstrate that ZrB_2 retains its primary hexagonal crystalline structure even after exposure to high gamma doses, which confirms its high radiation resistance. No new phases or pronounced oxide phases were detected by XRD, although small peak shifts and slight lattice expansion indicated the presence of local lattice distortions and weak amorphization effects. FTIR analysis revealed dose-dependent enhancement of bands related to Zr–O–Zr, Zr–O, and Zr–O–C bonds, showing that irradiation promotes the formation of active surface oxidation-related centers. Positron annihilation spectroscopy confirmed substantial changes in the defect structure, including an increase in positron lifetime components and redistribution of trapping centers, which is associated with the formation and evolution of vacancy-type defects and intergranular defect regions. The S and W parameter trends, together with electron momentum distribution results, further supported the conclusion that gamma irradiation modifies both the defect concentration and the local electronic structure of ZrB_2. Thermal annealing contributed to structural stabilization and promoted a tendency toward a more equilibrium defect configuration. Therefore, zirconium diboride can be considered a structurally stable and radiation-tolerant ceramic material with strong potential for applications in environments exposed to high gamma radiation.

Author Contributions. S.S. (Samadov Samir) performed the formal analysis, prepared the original draft of the manuscript, reviewed and edited the manuscript, and supervised the research. N.M.T. (Nguyen Minh Trung) contributed to the validation of the results, data visualization, and preparation of the original draft of the manuscript. E.P. (Evgeni Popov) performed the formal analysis and contributed to the review and editing of the manuscript. A.S. (Anatoliy Sidorin) contributed to the preparation of the original draft, reviewed and edited the manuscript, provided research resources, supervised the study, and approved the final version of the manuscript. All authors have read and agreed to the published version of the manuscript.
Funding. Not applicable.
Data Availability. The data supporting the findings of this study are available from the corresponding author upon reasonable request.
Declarations
Conflict of Interest. The authors declare no conflict of interest.
Competing Interests. The authors declare that they have no competing interests.
Ethical Approval. This article does not involve studies with human participants or animals. Therefore, ethical approval was not required.
Informed Consent. Not applicable.
Acknowledgment. The authors gratefully acknowledge the support and research facilities provided by the Joint Institute for Nuclear Research (JINR), Dubna, Russian Federation.

References

[1] Monteverde F, Bellosi A, Scatteia L. Processing and properties of ultra-high temperature ceramics for space applications. Materials Science and Engineering A. 2008;485(1–2):415–421. https://doi.org/10.1016/j.msea.2007.08.054
[2] Kalavathi V, Bhuyan RK. A detailed study on zirconium and its applications in manufacturing process with combinations of other metals, oxides and alloys: A review. Materials Today: Proceedings. 2019;19:781–786. https://doi.org/10.1016/j.matpr.2019.08.130

[3] Li H, Zhang L, Zeng Q, Wang J, Cheng L, Ren H, Guan K. Crystal structure and elastic properties of ZrB compared with ZrB_2: A first-principles study. Computational Materials Science. 2010;49(4):814–819. https://doi.org/10.1016/j.commatsci.2010.06.027
[4] Loftus N, Olivares J, Crespillo M, Pérez EE, Watts J, Bohannan E, Hilmas GE, Fahrenholtz WG, Graham JM. Microstructural evolution of zirconium diboride irradiated with 5–10 MeV Au ions at room temperature and 570 °C. Journal of the European Ceramic Society. 2026;46:117902. DOI: to be assigned.
[5] Lin YR, Koyanagi T, Sprouster DJ, Petrie CM, Fahrenholtz WG, Hilmas GE, Katoh Y. Response of ^{11}B-enriched ZrB_2 ultra-high temperature ceramic to neutron irradiation at elevated temperatures. Acta Materialia. 2024;276:120111. DOI: to be assigned.
[6] Astecker T, Hosemann P, Balooch M, Lee AN, Crespillo ML, Hattar K, Liedke MO, Wagner A, Polcik P, Kirnbauer A, Mayrhofer PH. Influence of helium ion irradiation on the mechanical properties of high-entropy (Hf,Ta,Ti,V,Zr)-nitride, -carbide and -diboride thin films: A comparative study. Materials & Design. 2025;256:114223. DOI: to be assigned.
[7] Monteverde F, Guicciardi S, Bellosi A. Advances in microstructure and mechanical properties of zirconium diboride-based ceramics. Materials Science and Engineering A. 2003;346:310–319.
[8] Magnuson M, Tengdelius L, Greczynski G, Hultman L, Högberg H. Chemical bonding in epitaxial ZrB_2 studied by X-ray spectroscopy. Thin Solid Films. 2018;649:89–96.
[9] Paxton WA, Özdemir TE, Şavklıyıldız E. Anisotropic thermal expansion of zirconium diboride: An energy-dispersive X-ray diffraction study. Journal of Ceramics. 2016;2016:8346563.
[10] Zhang M, Ma X, Yin J, Zhang Y, Zhang L, Wen J, Dai L, Kuang R, Chen H, Weng X, Zhao X, Liang D, Xie J, Deng L. Microstructure, infrared optical properties and thermal stability of ZrB_2 and double-layer-structure Al_2O_3/ZrB_2 thin films by magnetron sputtering technique. Applied Surface Science. 2020;532:147280.
[11] Karwasz GP, Zecca A, Brusa RS, Pliszka D. Application of positron annihilation techniques for semiconductor studies. Journal of Alloys and Compounds. 2004;382(1–2):244–251. https://doi.org/10.1016/j.jallcom.2004.04.080
[12] Demir E, Mirzayev MN, Popov EP, Horodek P, Genov IG, Siemek K, Mirzayeva DM, Turchenko VA, Bulavin M, Beskrovnyi AI, Valizade AH, Akhundzada HV, Karaaslan SI. Effects of high-energetic $^{3}He^{+}$ ion irradiation on tungsten-based composites. Vacuum. 2021;184:109934. https://doi.org/10.1016/j.vacuum.2020.109934
[13] Mirzayev MN. High-flux neutron irradiation of boron trioxide analyzed with Raman and FTIR spectroscopy. International Journal of Modern Physics B. 2020;34(30):2050160. https://doi.org/10.1142/S0217979220501604
[14] Kansy J. Microcomputer program for analysis of positron annihilation lifetime spectra. Nuclear Instruments and Methods in Physics Research Section A. 1996;374(2):235–244. https://doi.org/10.1016/0168-9002(96)00075-7
[15] Dryzek J. Research activities on positron annihilation spectroscopy. Institute of Nuclear Physics, Polish Academy of Sciences (IFJ PAN). Available from: https://ifj.edu.pl
[16] Blumenthal H, Norton JT, Sindeband SJ. Structures of diborides of titanium, zirconium, columbium, tantalum and vanadium. Transactions of the American Institute of Mining, Metallurgical and Petroleum Engineers. 1949;185:749–751.
[17] Bao W, Robertson S, Zhao JW, Liu JX, Wu H, Zhang GJ, Xu F. Structural integrity and damage of ZrB_2 ceramics after 4 MeV Au ions irradiation. Journal of Materials Science & Technology. 2021;72:223–230. https://doi.org/10.1016/j.jmst.2020.08.058
[18] Abiyev AS, Huseynov EM, Hashimov RF. Gamma radiation-induced alterations in nanocrystalline titanium nitride (TiN) particles: A structural perspective. Radiation Physics and Chemistry. 2024;218:111638. https://doi.org/10.1016/j.radphyschem.2024.111638

[19] Han JS, An GS, Choi S. Synthesis of ZrB_2@SiC composite particles through sol–gel and carbothermal reduction. Materials Today Communications. 2022;33:104646. https://doi.org/10.1016/j.mtcomm.2022.104646
[20] Cheng YH, Qi Y, Hu P, Zhou S, Chen G, An J, Jin K, Han W. ZrB_2–SiC–G composite prepared by spark plasma sintering of in situ synthesized ZrB_2–SiC–C composite powders. Journal of the American Ceramic Society. 2016;99(6):2131–2137. https://doi.org/10.1111/jace.14207
[21] Li Y, Chen S, Ma X, et al. A simple way to prepare a precursor for ZrC–SiC ceramics. Journal of Materials Science. 2016;51:5160–5169. https://doi.org/10.1007/s10853-016-9807-3
[22] Bhaskar S, Awin EW, Kumar KCH, et al. Design of nanoscaled heterojunctions in precursor-derived t-ZrO_2/SiOC(N) nanocomposites: Transgressing the boundaries of catalytic activity from UV to visible light. Scientific Reports. 2020;10:430. https://doi.org/10.1038/s41598-019-57270-8
[23] Yabuuchi A, Tanaka M, Kinomura A. Radiation effects in materials studied by positron annihilation. Journal of Nuclear Materials. 2020;542:152473. https://doi.org/10.1016/j.jnucmat.2020.152473
[24] Stewart DM, Meulenberg RW, Lad RJ. Surface and interface studies in thin films. Thin Solid Films. 2015;596:155–159. https://doi.org/10.1016/j.tsf.2015.10.002
[25] Zhu Z, Yao M, Shi J, Yao C, Lu E, Cao X, Wang B, Wu Y. Radiation-induced defects in materials. Journal of Nuclear Materials. 2018;508:12–19. https://doi.org/10.1016/j.jnucmat.2018.05.022
[26] Brusa RS, Macchi C, Mariazzi S, Karwasz GP. Positron annihilation studies in materials science. Acta Physica Polonica A. 2005;107(5):702–711. https://doi.org/10.12693/APhysPolA.107.702
[27] Cizek J, Melikhova O, Prochazka I, Kuriplach J, Kuzel R, Brauer G, Anwand W, Konstantinova TE, Danilenko IA. Defect studies of nanocrystalline zirconia powders and sintered ceramics. Physical Review B. 2010;81:024116. https://doi.org/10.1103/PhysRevB.81.024116
[28] Tuomisto F, Makkonen I. Defect identification in semiconductors with positron annihilation: Experiment and theory. Reviews of Modern Physics. 2013;85(4):1583–1631. https://doi.org/10.1103/RevModPhys.85.1583
[29] Zhang S, Schut H, Brück E, van der Zwaag S, van Dijk NH. Effect of carbon on copper precipitation in deformed Fe-based alloys studied by positron annihilation spectroscopy. Journal of Physics: Conference Series. 2013;443:012027. https://doi.org/10.1088/1742-6596/443/1/012027
[30] Pujari PK, Sudarshan K, Goswami A, Manohar SB. Positron annihilation studies in the MgB_2 superconductor. Physical Review B. 2002;66:012518. https://doi.org/10.1103/PhysRevB.66.012518